
*Photosensitive characteristics of ambient Aerosol in the Maritime
environ*

Nwobi Obi Somtochukwu

Institute of Maritime studies, University of Nigeria Nsukka.

Obi.nwobi@unn.edu.ng

Abstract

Systematic characterization of aerosol over the oceans is needed to understand the aerosol effect on climate and on transport of pollutants between continents. Reported are the results of a comprehensive photosensitive (optical) and physical characterization of ambient aerosol in five key island locations of the Aerosol Robotic Network (AERONET) of sun and sky radiometers, spanning over 2–5 yr. The results are compared with aerosol optical depths and size distributions reported in the literature over the last 30 yr. Aerosol found over the tropical Pacific Ocean (at three sites between 208S and 208N) still resembles mostly clean background conditions dominated by maritime aerosol. The optical thickness is remarkably stable with mean value of $t_a(500\text{ nm}) \approx 0.07$, mode value at $t_{am} \approx 0.06$, and standard deviation of 0.02–0.05. The average Ångström exponent range, from 0.3 to 0.7, characterizes the wavelength dependence of the optical thickness. Over the tropical to subtropical Atlantic (two stations at 78S and 328N) the optical thickness is significantly higher: $t_a(500\text{ nm}) \approx 0.14$ and $t_{am} \approx 0.10$ due to the frequent presence of dust, smoke, and urban–industrial aerosol. For both oceans the atmospheric column aerosol is characterized by a bimodal lognormal size distribution with a fine mode at effective radius $R_{eff} \approx 0.11 \pm 0.01\text{ }\mu\text{m}$ and coarse mode at $R_{eff} \approx 2.1 \pm 0.3\text{ }\mu\text{m}$. A review of the published 150 historical ship measurements from the last three decades shows that t_{am} was around 0.07 to 0.12 in general agreement with the present finding. The information should be useful as a test bed for aerosol global models and aerosol representation in global climate models. With global human population expansion and industrialization, these measurements can serve in the twenty-first century as a basis to assess decadal changes in the aerosol concentration, properties, and radiative forcing of climate.

1. Introduction

Aerosol science returned to prominence in the last decade due to clear evidence of anthropogenic impacts and the important role of aerosols in the radiative forcing of climate. It became evident that in order to understand the effect of greenhouse gases

on past climates and on future climate change (e.g., Hansen et al. 2000) we need accurate information on aerosol optical properties (Penner et al. 1994) and their direct and indirect (through cloud modification) interaction with the solar and thermal radiation (Twomey 1984; Charlson et al. 1992; IPCC 1994). The variety of



aerosol sources both natural and anthropogenic, and the short lifetime of aerosols (5–10 days) results in a spatially and temporally heterogeneous aerosol field, making aerosol characterization and modeling a real challenge. To characterize this diversity there have been a flurry of field experiments in the last decade [e.g., heavy smoke aerosol in South America—Smoke, Clouds, and Radiation-Brazil (Kaufman et al. 1998); pollution from the eastern United States—Tropospheric Aerosol Radiative Forcing Observational Experiment (Russell et al. 1999); clean maritime aerosol—First Aerosol Characterization Experiment (Bates et al. 1998a); Atlantic aerosol—Second Aerosol Characterization Experiment (Raes et al. 2000); and recently heavy mixed aerosol in the Indian Ocean—Indian Ocean Experiment (Ramanathan et al. 2001); and southern Africa—Southern Africa Fire-Atmosphere Research Initiative] development of new satellite instrumentation (King et al. 1999), consistent analysis of historical satellite records (Jankowiak and Tanre 1992; Husar et al. 1997; Herman et al. 1997; Mishchenko et al. 1999) and development of ground-based networks of radiometers for systematic and accurate long-term measurements (Holben et al 1998, 2001).

The basic philosophy is that once these datasets are incorporated into aerosol and climate models in a consistent manner or used for their validation, we shall be able to better understand the role of aerosol in climate and improve the prediction of future changes (e.g., Kiehl and Briegleb 1993; Hansen et al. 1997). Without a comprehensive assessment of present aerosol concentrations and optical properties, we shall not be able to measure the change in the aerosol radiative forcing, and thus of the impact of changes of human activity on climate.

Field experiments provide the most comprehensive analysis of aerosol properties and their radiative impact [e.g., the comprehensive analysis of all aerosol impacts in the Indian Ocean by Ramanathan et al. (2001)] but they are limited in temporal and geographical extent. Satellites monitor the whole globe on a daily or weekly basis, and can generate long-term data sequences, but satellites derive aerosol information from the scattered light over varying terrain properties, and thus are limited in their information content and accuracy (e.g., Tanre´ et al. (1996). Remote sensing from ground-based sun– sky radiometers measures both the spectral



attenuation of sunlight and the spectral-angular properties of scattered light—sky brightness. These measurements provide the most accurate and comprehensive long-term measurements of the optical properties of the ambient aerosol (Holben et al. 2001; Dubovik et al. 2002) in the entire atmospheric column, in specific instrumented locations.

In the current paper we analyze atmospheric aerosol optical properties using 2–5 yr of measurements by the Aerosol Robotic Network (AERONET) in five island locations in the Pacific and Atlantic Oceans. The AERONET solar attenuation and sky brightness measurements are used to derive the spectral optical thickness and size distribution of the column ambient aerosol. In contrast to in situ measurements, AERONET remote measurements do not characterize the aerosol chemical composition, but measure the optical properties of the aerosol, unaffected by sampling and drying processes inherent in in situ methods. The AERONET measurements are compared with a comprehensive survey of shipborne measurements published over the last 30 yr.

2. Historical overview

At the end of 1960s through the mid-1970s it became clear that our general knowledge of aerosol optical properties of the maritime atmosphere was very poor. Experimental data on aerosol optical properties above the oceans were scarce. Because of various reasons (data collection is very expensive, time and labor consuming, combined with instrumental and methodological difficulties) systematic experiments at sea were not conducted until the early 1980s. Since then significant progress has been made in the last 20 yr.

Table 1 summarizes the known published results of aerosol optical depth measurements in maritime and coastal areas. Unfortunately, numerous experiments were neither systematic nor extensive, employed only a few wavelengths, and measurement accuracy sometimes was unknown. However, the accumulated historical datasets can improve our understanding of aerosol optical depth spatial distributions, can become an important milestone in exploring the possibility of optical division into districts of the atmosphere above the oceans and establishing regional aerosol climatologies.



Data acquired over the Pacific Ocean indicate, generally, a more transparent atmosphere (small aerosol concentrations) as compared to the Atlantic Ocean, inland seas and coastal zones. Aerosol optical depth typically is low; however, long-range transport of dust from Asia during the spring months and global volcanic activity can increase the turbidity. Aerosol optical depth variability in remote oceanic areas is generally smaller than in the regions affected by continental sources. Spectral dependence of $t_a(\lambda)$ above the Pacific Ocean is more neutral than in coastal areas, owing to a large fraction of coarse-mode aerosol of sea origin (sea salt) in the size distribution.

Aerosol optical depth over the Atlantic Ocean shows large variability both temporally and spatially. It is greatly affected by the dust sources in Africa, pollutant sources in Europe and North America and biomass burning products in Africa and South America. Also, it can be noted that the spectral behavior of $t_a(\lambda)$ is more selective over the Atlantic than over the Pacific (higher Ångström parameter values correspond to generally higher extinction contributions from smaller particles). In the oceanic areas influenced

by Saharan dust high turbidity [high $t_a(\lambda)$] corresponds to small values of Ångström parameter a , since in that case large particles of nonmaritime origin (dust) are dominant.

There is very little aerosol data for the Indian Ocean. Only recently an extensive field experiment measured the properties of aerosol in that region (Ramanathan et al. 1995). Aerosol optical depth is typical of background ocean values in the remote areas of the South Indian Ocean [south from the intertropical convergence zone (ITCZ)] (Matsubara 1983; Barteneva et al. 1991). The high $t_a(\lambda)$ in the Arabian Sea and areas close to Africa are associated with mineral dust, advected from Saudi Arabia, Iraq, southern Iran, and East Africa, and pollution aerosols from southwestern coast of India. The seasonality of the aerosol transport and relatively short period during ship cruises did not permit establishment of intraannual seasonal patterns in a majority of publications except for a paper by Moorthy and Satheesh (2000). Based on a 2-yr record they outlined the role of seasonally changing air mass type in causing a regular annual variation in spectral optical depths (t_a ranges from 0.20 to 0.50 at a wavelength 500 nm).



3. Data collection

Aerosol optical properties were derived from direct sun and sky radiation measurements performed at the operational AERONET sites in the Pacific (Nauru, Lanai, Tahiti) and in the Atlantic (Bermuda, Ascension Island; Fig. 1).

The island of Nauru (08309S, 1668549E) is situated in the tropical western Pacific Ocean. The island is very small with a total land area ;25 km². It lies ;40 km south of the equator and the nearest neighbor island is 300 km away. Nauru is a good example of an equatorial oceanic site and was chosen by the Atmospheric Radiation Measurement Program to set up a Cloud and Radiation Testbed site (Mather et al. 1998).

The island of Lanai (208499N, 1568599W) is situated in the tropical Pacific Ocean. It is a part of the Hawaiian Islands. Lanai has a total land area of ;365 km², and is more than 3500 km away from the nearest continental landmass (California coast). Therefore, air that reaches it, regardless of source, spends enough time over the ocean to be considered “truly maritime.” Long-distance high-altitude dust transport from Asia is an only exception. Because of the shelter

provided by the surrounding islands, Lanai receives very little rain and is not known for large waves (Price 1983).

Tahiti is the largest island in French Polynesia. It is situated in the eastern South Pacific at 178329S, 1498349W. Tahiti has a total land area of ;1000 km² and is 5400 km away from the nearest continent (Australia). The tropical climate has two distinct seasons here, wet season, between November and April, and dry season, between May and October.

Bermuda is an archipelago of seven islands situated in the western North Atlantic Ocean, approximately 1050 km from Cape Hatteras (North Carolina, U.S. east coast). Climate on Bermuda is subtropical with no wet season. Air that reaches Bermuda cannot always be considered truly maritime. One can observe three different optical conditions associated with various aerosol sources, which are defined in terms of generalized source trajectories: pure Atlantic air, air from North America, and Saharan dust (Reddy et al. 1990; Smirnov et al. 2000a). A sun photometer was located at the Bermuda Biological Station (328229N, 648419W).



The small island of Ascension is situated in the South Atlantic (078569S, 148229W) and covers an area of ;80 km². Ascension is a rocky peak of purely volcanic origin. The climate is tropical. Dust and biomass burning aerosols from Africa reach Ascension Island. Although such occurrences are sporadic they affect the optical properties over the island.

All of the measurements reported in this paper were made with the automatic sun and sky scanning radiometers CIMEL. Three of the instruments deployed (Lanai, Tahiti, and Ascension) were CIMEL radiometers belonging to the Sensor Intercomparison and Merger for Biological and Interdisciplinary Oceanic Studies project (McClain and Fargion 1999). Four instruments (Nauru, Lanai, Tahiti and Ascension) were reengineered. The reengineering included a number of modifications to “harden” the sun–sky radiometer for deployments in corrosive marine environments.

The CIMEL radiometers made measurements of the direct sun and diffuse sky radiances within the spectral range 340–1020 nm and 440–1020 nm, respectively (Holben et al. 1998). The direct sun measurements are acquired in eight

spectral channels at 340, 380, 440, 500, 670, 870, 940, and 1020 nm (nominal wavelengths). Seven of the eight bands are used to acquire aerosol optical depth data. The eighth band at 940 nm is used to estimate total precipitable water content. The bandwidths of the ion-assisted deposition interference filters employed in the CIMEL radiometer vary from 2–4 nm (UV channels) to 10 nm for visible and nearinfrared channels.

Holben et al. (1998) and Eck et al. (1999) presented careful assessments of the overall uncertainty in computed t_a due to calibration uncertainty, lack of surface pressure data and actual ozone column amount. Typically, the total uncertainty in $t_a(l)$ for a field instrument is ;Dt_a 5 60.01 to 60.02, and is spectrally dependent with the higher errors (60.02) in the UV spectral range. Schmid et al. (1999) showed that discrepancies between aerosol optical depths measured by a CIMEL radiometer and four other radiometers in field experimental conditions were within 0.015 (rms). The details of the water vapor content (WVC) retrieval procedure and the types of errors involved can be found in Schmid et al. (2001). An automatized and computerized cloud-screening algorithm



(Smirnov et al. 2000b) was applied to the direct sun measurements.

The sky radiance almucantar measurements are acquired in four spectral channels at 440, 670, 870, and 1020 nm. For each solar zenith angle sky radiances are taken at 28 azimuth angles within the relative azimuth angle range (from the sun) of 28–180° (Holben et al. 1998). A flexible inversion algorithm for retrieval of aerosol optical properties, developed by Dubovik and King (2000), was used for retrieving aerosol volume size distributions over a range of radii from 0.05 to 15 μm together with spectrally dependent complex refractive index and single scattering albedos from spectral sun and sky radiance data. An inversion strategy, details of the algorithm development and the methodological aspects of a detailed statistical optimization of the influence of noise in the inversion procedure are discussed in depth in (Dubovik and King 2000).

The accuracy of the retrieved aerosol particle size distributions and single scattering albedos (SSA) has been studied in detail by Dubovik et al. (2000). Retrieval errors in $dV/d \ln R$ typically do not exceed 15% for water-soluble aerosol type for each

particle radius within the 0.1–7-μm range. The errors for very small particles (r ; 0.05–0.1 μm) and very large particles (r ; 7–15 μm) may be as large as 15%–100% (for each particle radius bin). However, no significant shifts in the positions of mode radii or changes in the shape of size distributions are expected. Single scattering albedos (SSAs) are expected to have an uncertainty of 0.05–0.07 for water soluble aerosol type and when $t_a(440 \text{ nm}) > 0.20$ (Dubovik et al. 2000).

For simplicity we will characterize the atmospheric aerosol optical properties by two parameters: $t_a(500 \text{ nm})$, which is the aerosol optical depth at a wavelength 500 nm, and the Ångström parameter a , derived from a multispectral log–linear fit to the classical equation $t_a \propto \lambda^{-2a}$ (based on 4 wavelengths in the range 440–870 nm). Although not all optical depth spectra are well represented by an Ångström fit (see e.g., Knestrick et al. 1962; King and Byrne 1976; Kaufman 1993; Villevalde et al. 1994; Eck et al. 1999; O'Neill et al. 2001), a can still be considered as a first-order parameter indicative of the general size distribution and the relative dominance of fine- versus coarse-mode particles. It is noted that for bimodal size distributions with



a significant coarse-mode and coarse-mode-dominated size distributions the spectral curvature of $\ln t_a$ versus $\ln l$ is very small (Eck et al. 1999).

4. Results

a. Aerosol optical depth statistics

The significant number of the data sources considered in Table 1 gave an opportunity to evaluate the real variability of aerosol optical depth and A_{ngstrom} parameter for various regions. One can observe that the largest optical variability occurs in the Atlantic Ocean. This high degree of variability is largely attributable to the diverse contributions of a variety of continental aerosol sources (urban-industrial, dust, and biomass burning). The enrichment of maritime air by “stationary” and “fresh” sea-spray aerosol components (Gathman 1983) is an additional source of variability. We estimate that the combination of five datasets considered in the current study (three over the Pacific and two over the Atlantic) is sufficient for the characterization of the background optical conditions over the oceans in the tropical and subtropical regions.

Table 3 summarizes measurements of aerosol optical depth in oceanic areas for which analyses have been performed in the current study. One can observe indications of differences between Pacific and Atlantic sites in terms of the aerosol optical depth value as well as the A_{ngstrom} parameter. As would be expected, optical depth is higher over the Atlantic sites (mixed maritime aerosol type) than over the Pacific. The smaller mean A_{ngstrom} value over Nauru as compared to the other sites may be attributed, in the first instance, to the smallest island area and to different degree of sea-spray production and deposition.

The mean $t_a(500 \text{ nm})$ values of 0.07–0.08 for the Pacific sites are close to the results presented by Masuda et al. (1999), Quinn (1995, unpublished data), Clarke and Porter (1994), Volgin et al. (1988), and Shaw (1983) (see Table 1). Standard deviation (s) of 0.02–0.03 is an

standard deviation of the aerosol optical depth.

a and a_m mean and mode values of the A_{ngstrom} parameter. s_a , standard deviation of the A_{ngstrom} parameter. The value of $s \approx 0.02$ was reported by Volgin et al. (1988) based on a series of 48 measurements in the Pacific. The

TABLE 3. Statistical characteristics of aerosol optical depth and Ångström parameter a.

Site	Time period	N ^a	Aerosol type	t_{500}	t_{550}	t_{650}	t_{870}	t_{1020}	t_{1240}	t_{1640}
Lanai, Pacific Ocean	Nov 1995–Apr 2000	722	Maritime	0.07	0.05	0.76	0.37	0.06	0.70	
Nauru, Pacific Ocean	2000	276	Maritime	0.08	0.03	0.43	0.35	0.06	0.30	
Tahiti, Pacific Ocean	Jun 1999–Apr 2000	234	Maritime	0.07	0.02	0.74	0.27	0.06	0.70	
Bermuda, Atlantic Ocean	2000	590	Mixed	0.14	0.09	0.93	0.41	0.09	0.90	
Ascension, Atlantic Ocean	Jul 1999–May 2000	338	maritime	0.13	0.07	0.62	0.30	0.11	0.70	
	Mar 1996–Dec 1999		Mixed							
	Nov 1998–Jun 2000		maritime							

^a N, number of analyzed days. ^b t_a and t_{am} mean and mode values of aerosol optical depth at a wavelength 500 nm.

mean a value of 0.43 at Nauru is close to the values of 0.56 and 0.45 reported by Villevalde et al. (1994) and Volgin et al. (1988) for the Pacific.

The mean $t_a(500\text{ nm})$ values of 0.13–0.14 for the two AERONET Atlantic sites differ almost by a factor of 2 from the Pacific AERONET data. This value agrees with the results reported by Reddy et al. (1990), Hoppel et al. (1990), Ignatov et al. (1993), Korotaev et al. (1993), and Smirnov et al. (1995b, 2000a) (see Table 1) within one standard deviation. The larger variability of optical properties over Bermuda and Ascension caused standard deviation to increase by a factor of 2, at least, compared

to the clean remote maritime conditions in the Pacific. The mean value of the Ångström parameter at Bermuda (0.93) is higher than over the Pacific sites, but very close to the values reported by Hoppel et al. (1990), Reddy et al. (1990), Villevalde et al. (1994), and Smirnov et al. (1995a,b) for the Atlantic.

Figure 2a illustrates the daily averaged aerosol optical depth at 500 nm for Nauru. Daily average values show small day-to-day variation. Computed standard deviations of daily $t_a(500\text{ nm})$ range from below 0.01 to 0.05 (Fig. 2b). The Ångström parameter a showed that coarse particles (small a) almost always influence atmospheric aerosol optical properties



above Nauru (Fig. 2c). The values of which are typically less than 0.5 indicate the presence of coarse-mode sea-salt aerosol. Mean daily values of the WVC are, generally, between 3 and 6 cm of precipitable water (Fig. 2d) with no intraannual signature over the data interval.

Daily mean values of $t_a(500 \text{ nm})$ over Lanai (Fig. 3a) show the spring seasonal peaks. The seasonal variation of the monthly average aerosol optical depth showed maximum in the spring season months (March, April, and May) (Holben et al. 2001). This seasonal peak in spring is due to the long-ranged transport of Asian aerosols (Shaw 1980; Bodhaine et al. 1981). Perry et al. (1999) suggested that the long-range transport of biomass burning aerosols from Mexico and Central America could affect optical conditions over Hawaii.

Daily variations are also due in part to variation in the production and transport of volcanic aerosols from the active volcanoes on the island of Hawaii. Computed standard deviations of daily $t_a(500 \text{ nm})$ generally are less than 0.04 (Fig. 3b). The Ångström parameter a showed larger variability than over Nauru (Fig. 3c). Daily average water vapor contents (Fig. 3d) range from less than 2 cm to 5 cm and exhibit some

seasonality with higher values in the summer.

Elimination of the spring (March, April, May) data (influenced by possible dust and volcano aerosol contamination) from the Lanai dataset did not change mode values of the optical parameters. Further analysis performed by Kaufman et al. (2001) derived optical properties of the baseline aerosol, that are very close to the results reported in the current study.

Daily averages of $t_a(500 \text{ nm})$ over Tahiti and its standard deviations are shown in Figs. 4a and 4b, respectively. Day-to-day variability is low, indicating a relative stability of optical properties. In the majority of cases the computed standard deviations of daily $t_a(500 \text{ nm})$ range below 0.03 (Fig. 4b). The Ångström parameter a (Fig. 4c) showed smaller variability than over Lanai and Nauru. The daily average values of the water vapor content (Fig. 4d) show higher values in the summertime (December, January, February). This is consistent with the general synoptic pattern for the area.

Figure 5a presents the daily averaged aerosol optical depth at 500 nm for the measurement period over Bermuda. The aerosol optical depth for this site is higher in



the summertime (see also Holben et al. 2001), which is associated Standard deviations of daily $t_a(500 \text{ nm})$ range generally below 0.03, however, occasionally can far exceed this value (Fig. 5b). Daily average values of a show significant variability and large day to day variation (Fig. 5c). WVC exhibits a pronounced seasonal pattern with a maximum in July and August.

As previously mentioned dust and biomass burning aerosols from Africa can reach Ascension Island. However, the optical depth range and daily standard deviations (Figs. 6a and 6b) are smaller than over Bermuda.

The Ångström parameter is typically below 1 (Fig. 6c), which indicates that coarse particles (small a_s) usually dominate the aerosol optical properties. Therefore, atmospheric optical conditions on Ascension are closer to background maritime conditions in comparison to Bermuda.

The frequency of occurrence distributions for t_a and a are presented in Figs. 7 and 8. The frequency histograms of $t_a(500 \text{ nm})$ for the Pacific sites demonstrate that the majority of values (75%–85%) are less

than 0.10 (Figs. 7a–7c). The aerosol optical depth probability distributions for the Atlantic sites are relatively broader with the modal value of about 0.1. The most frequently occurring values of $t_a(500 \text{ nm})$ for all five sites are presented in Table 3.

The Ångström parameter frequency distribution for Nauru (Fig. 8) shows a relatively neutral spectral dependence of optical depth (modal value of $a ; 0.3$), for Lanai, Tahiti, and Ascension it has a peak around 0.7 with lesser frequencies trailing off at higher a values. The frequency histogram for Bermuda is slightly skewed towards higher a 's with peak frequency at 0.9. The mode a values are listed in Table 3.

The scattergrams in Fig. 9 demonstrates how daily averages of aerosol optical depth correlate with the Ångström parameter a in the five sites. For Nauru data a wide range of a at low aerosol optical depths ($r = -0.06$) and the high negative correlation ($r = -0.75$) between them, reflects the increasing influence of a background fine aerosol on $t_a(l)$ in a remote oceanic atmospheric conditions. One can observe a weak trend of increasing values of a as $t_a(500 \text{ nm})$ decreases over Tahiti. Correlation between them, however, cannot

be considered strong ($r = 0.2039$, i.e., only 15% of variance explained), thus indicating simply a reasonable trend. A variety of conditions are separated from urban-industrial aerosol cluster by relatively clean maritime conditions.

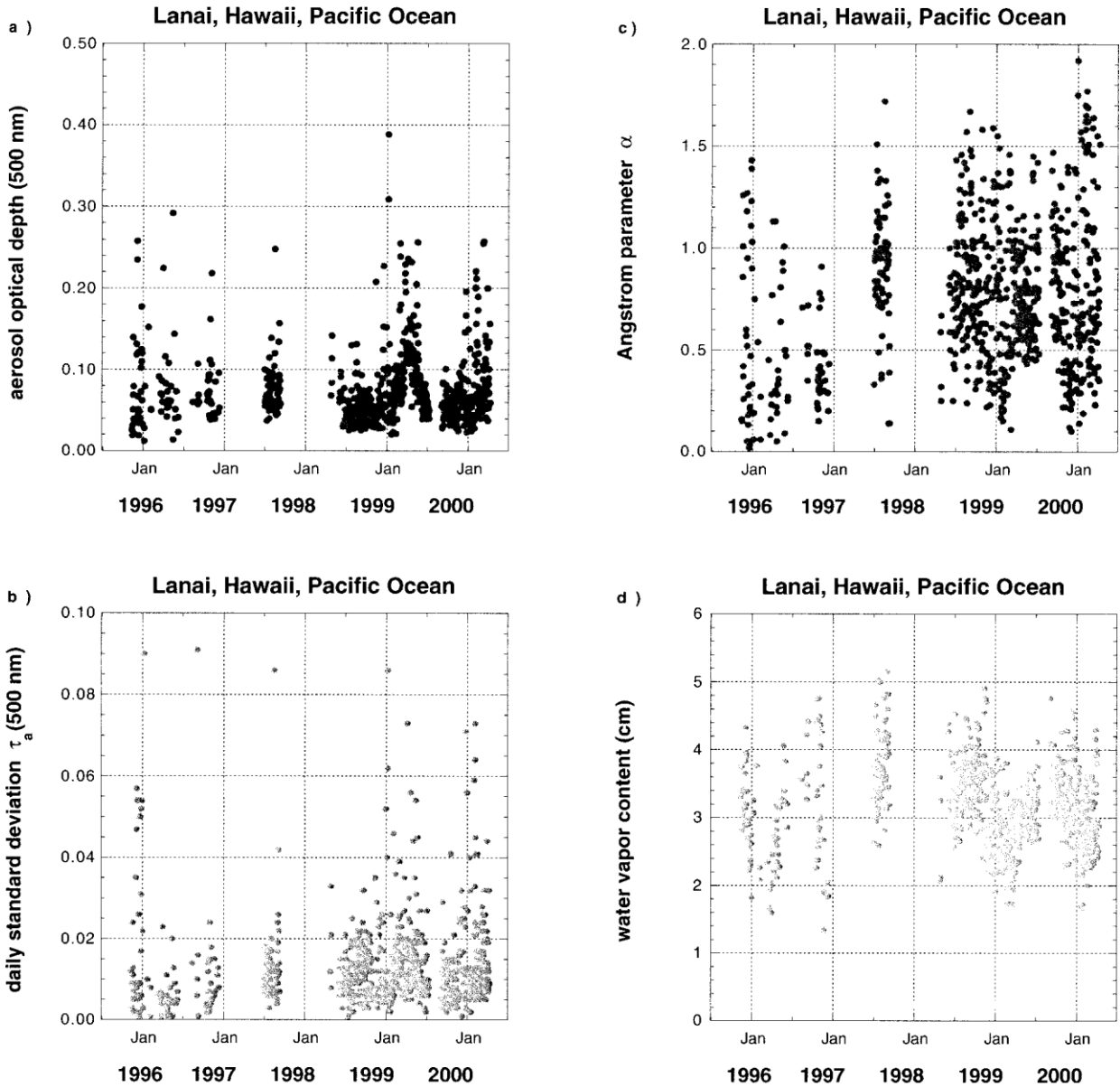


FIG. 3. Lanai, Hawaii (208499N, 1568599W; elevation 20 m), Pacific Ocean. (a) Mean daily values of aerosol optical depth at 500 nm, (b) daily std dev of $t_a(500 \text{ nm})$, (c) mean daily values of Angstrom parameter, and (d) WVC in the total atmospheric column.

optical conditions over Bermuda and Ascension can be seen in Fig. 9. Dusty



Aerosol volume size distributions and single scattering albedos in the total atmospheric column were retrieved from sun and sky radiance measurements according to Dubovik and King (2000). In the retrieval algorithm the aerosol particles are assumed to be polydisperse homogeneous spheres. Robustness of the retrieved size distributions was assured by the residual error threshold [see formula (6) in Dubovik et al. 2000] of less than 5% (between computed and measured radiances) and by the number of scattering angles in the measured sky radiance distributions not less than 21 (Dubovik et al. 2002).

Figure 10 illustrates averaged size amplitude and spectral shape of the optical

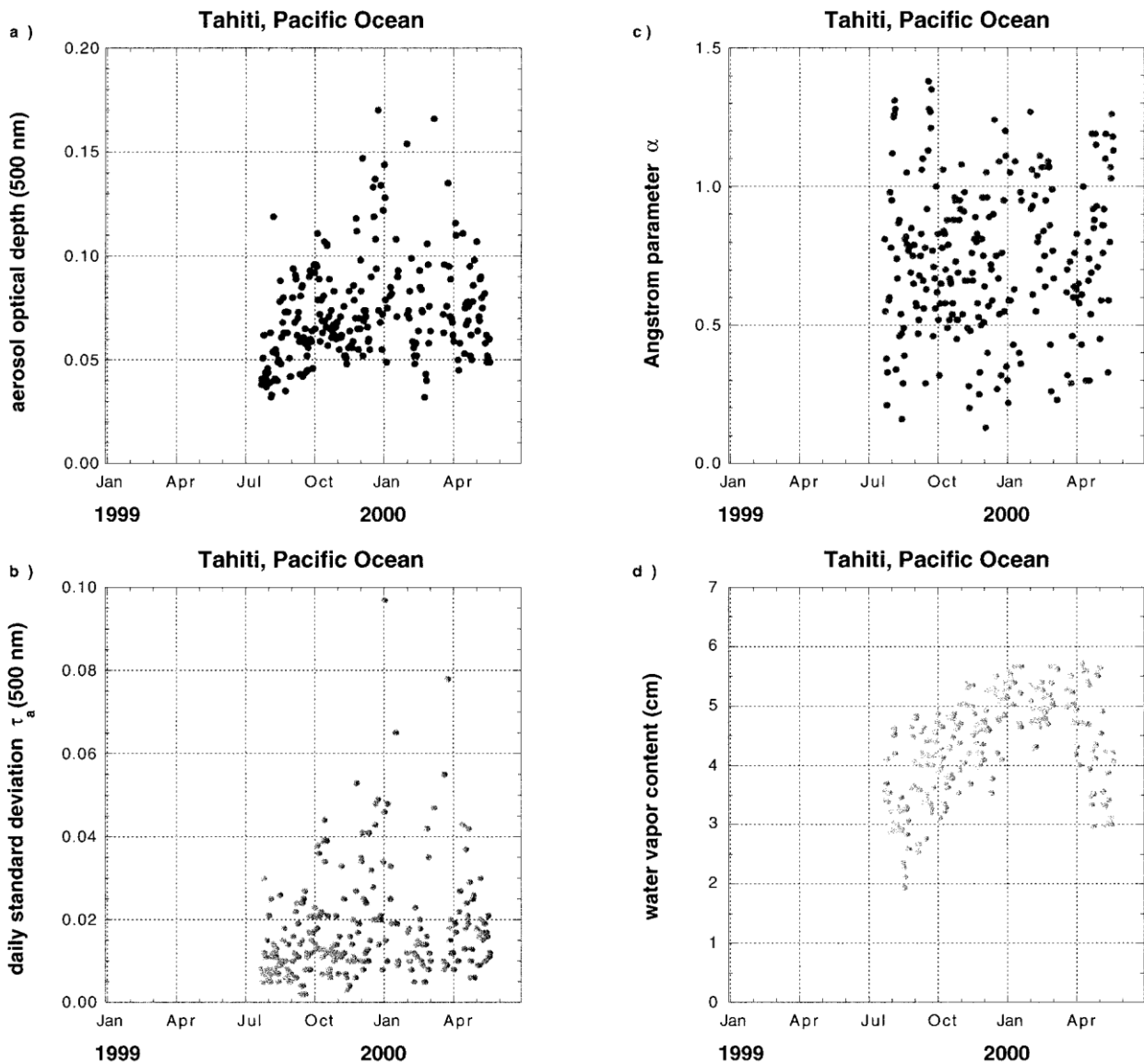


FIG. 4. As in Fig. 2 but for Tahiti (178329S, 1498349W; elevation 98 m), Pacific Ocean, $t_a(500$ nm).

distributions ($dV/d\ln R$) for the five sites considered. Two modes are evident, a fine mode with radius $r \approx 0.4$ μ m and a coarse mode with $r \approx 0.4$ μ m. The dominant variations in these distributions can be directly associated with changes in the

depth data [i.e., there is no significant influence of inversion artifacts due to nonspherisity (Dubovik et al. 2002)]. The volume size distributions in Fig. 10 clearly demonstrate the background natural aerosol optical properties over the Pacific



sites and modified maritime aerosols over the Atlantic. The wide variety of optical conditions changed the shape of the coarse aerosol fraction on Bermuda.

Table 4 presents parameters of the bimodal lognormal volume size distributions (Whitby 1978) shown in Fig. 10. It should be noted that we assigned particles with radii 0.05 μ m, 0.3 μ m, 0.4 μ m, 0.6 μ m and with radii 0.3 μ m, 4 μ m

0.6 μ m, 15 μ m to the fine and coarse modes respectively (before and after the inflection point). The effective radius is defined as a ratio of the third over the second moment of the size distribution. Volume concentrations for each fraction are also presented in Table 4.

Variations in aerosol volume size distributions over the Pacific were mainly due to changes in the concentration of the coarse aerosol fraction. Over the Atlantic the magnitude of the fine (accumulation) mode increased substantially, however, the relative contribution of the coarse mode is greater over Ascension than over Bermuda.

Parameters of the columnar aerosol size (0.2 μm). Retrieved values for the coarse-distributions listed in Table 4 are not mode radii are close to the models of

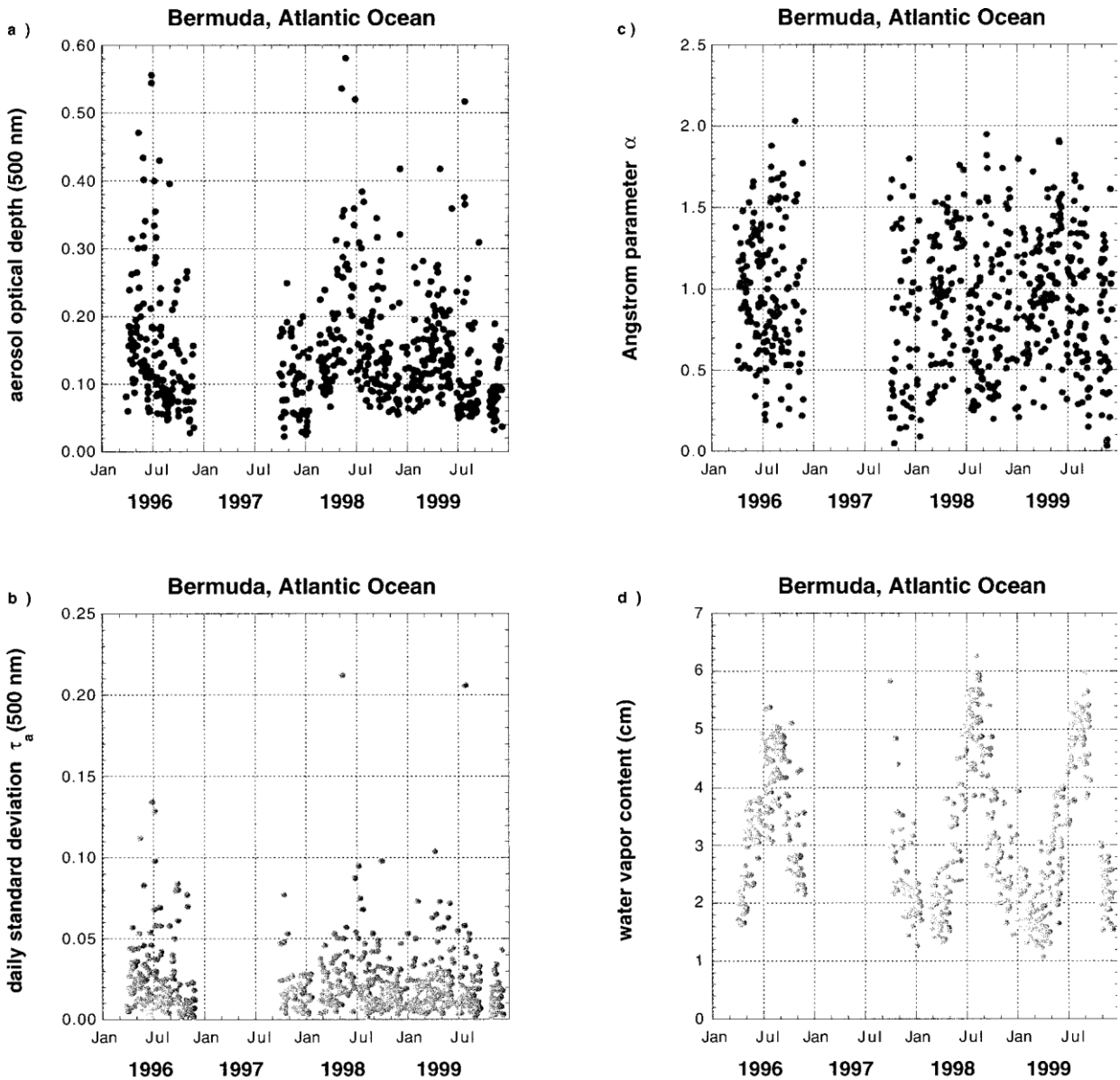


FIG. 5. As in Fig. 2 but for Bermuda (328229N, 648419W; elevation 10 m), Atlantic Ocean.

inconsistent with the results obtained in situ (e.g., Hoppel et al. 1985; Hoppel and Frick 1990; Hoppel et al. 1990; and Table 2). Agreement of the fine-mode geometric mean radii is rather remarkable (R_g ; 0.1–

Shettle and Fenn (1979), Porter and Clarke (1997), and the measurements of Horvath (1990), Kim et al. (1990), and Jennings et al. (1997). Measurement results reported by Quinn et al. (2001) for the Southern



Atlantic temperate air are also consistent with our retrievals. Note that parameters presented in Table 4 describe aerosol size distributions in ambient conditions and are not associated with particular relative humidity levels.

We have to admit that one would not expect the “dry” mode parameters to agree with either the ambient in situ measurements in Table 2 or the derived ambient size distributions in Fig. 10. It was not possible to adjust parameters presented for the “ambient” conditions in Table 2 to the so-called dry conditions, simply because the ambient relative humidity was not known. In case of the columnar size distribution retrievals it simply cannot be done. Dry radius of about 0.10 μm would be expected to be 0.14 μm for the “wet” (relative humidity ;90%) aerosol. For lower relative humidity (70% and 80%) the “humidity growth factor” is 1.06 and 1.22, respectively (Shettle and Fenn 1979).



Single scattering albedo retrievals were 0.01/0.10) is comparable with the inconclusive. SSA can hardly be retrieved absorption partition in total optical depth.

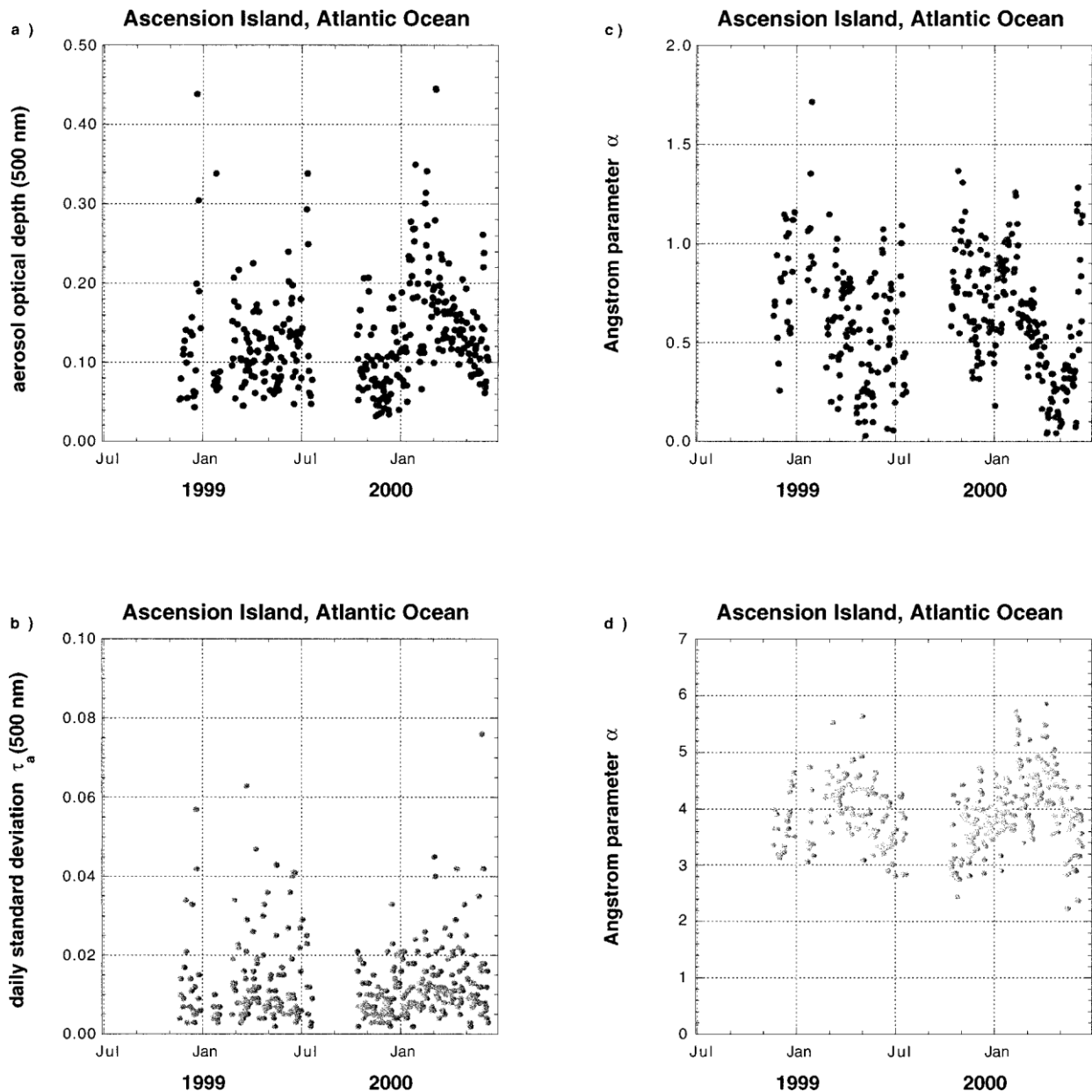


FIG. 6. As in Fig. 2, but for Ascension Island (78569S, 148229W; elevation 30 m), Atlantic Ocean.

in the conditions of low aerosol loading. Even the uncertainty of 60.01 in t_a for small $t_a \neq 0.10$ becomes More than 10% uncertainty in optical depth (in a sense of

5. Summary

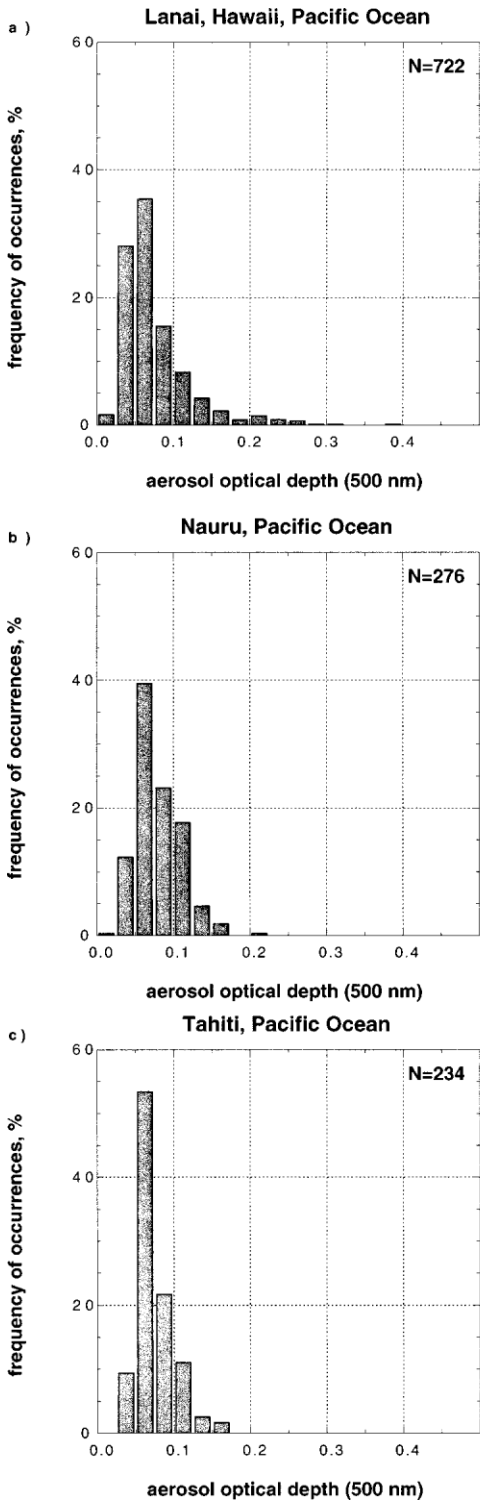
The principal conclusions drawn from our work can be summarized as follows.



1) A summary of aerosol optical depth measurements in a maritime environment during the last three decades was presented. The results of 75 publications were encapsulated in a single comprehensive table.

Despite instrumental and calibration differences overall, aerosol optical depths over remote oceanic areas (not influenced by desert dust outbreaks or volcanic activity) according to Table 1, are, as a rule, smaller than 0.12. In coastal areas and inland seas values of aerosol optical depth are higher, largely depending on continental sources. It is, however, noted that high-latitude oceanic data are underrepresented.

2) A short summary of the more recent in situ measurements of aerosol size distributions over the oceans was presented (Table 2). Parameters of aero-



(b) Nauru, (c) Tahiti, (d) Bermuda, and (e) Ascension Island.

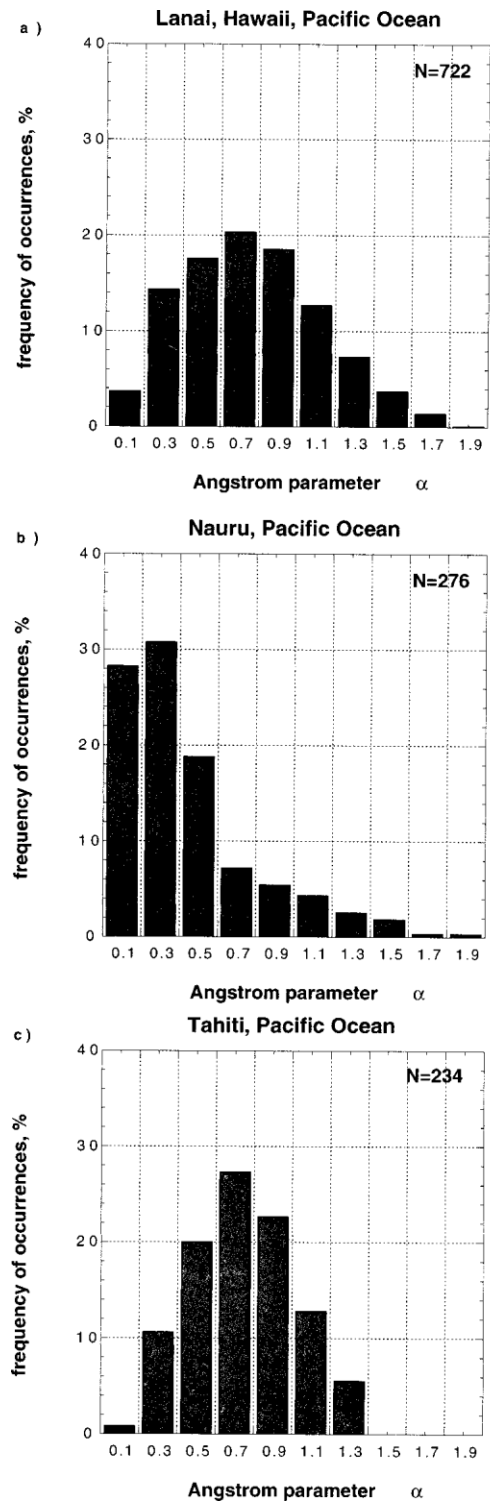


FIG. 7. Frequency of occurrences of aerosol optical depth at 500 nm for (a) Lanai,

FIG. 8. Frequency of occurrences of Angstrom parameter for (a) Lanai, (b) Nauru, (c) Tahiti, (d) Bermuda, and (e) Ascension Island.

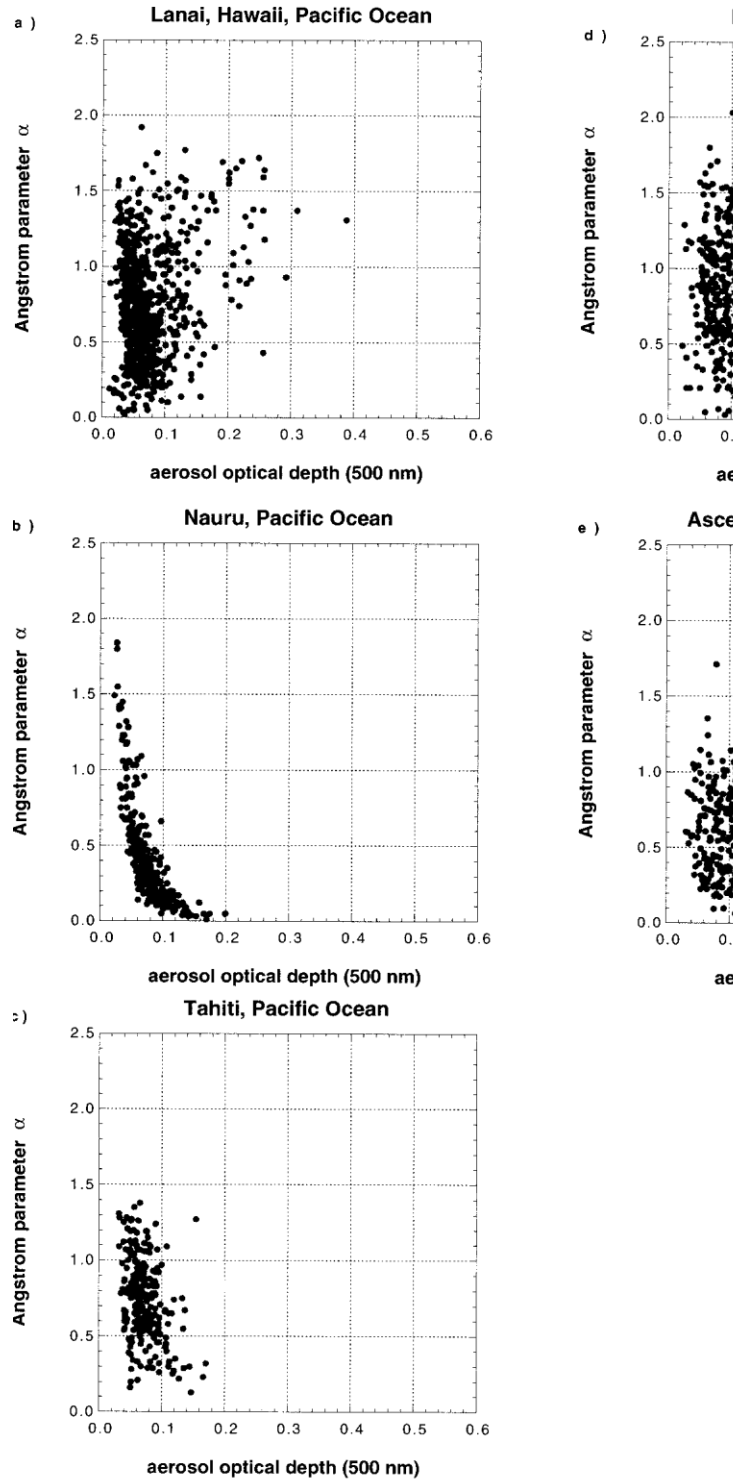


FIG. 9. Scattergrams of Angstrom parameter versus aerosol optical depth for (a)

Lanai, (b) Nauru, (c) Tahiti, (d)
Bermuda, and (e) Ascension
Island.

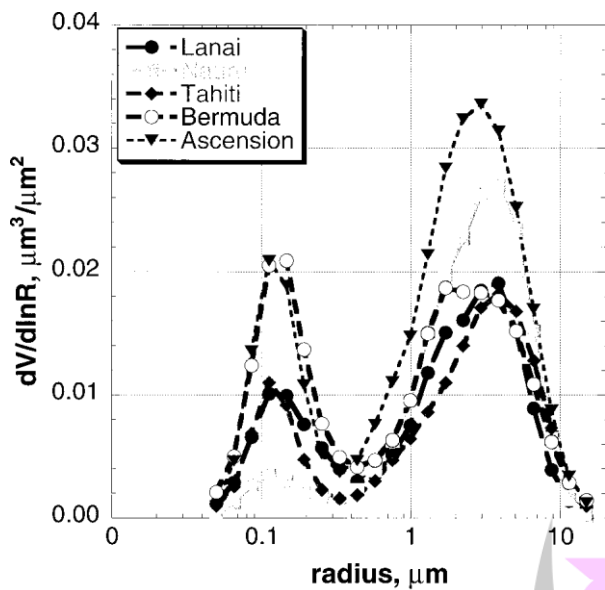


FIG. 10. Average aerosol volume size distributions in the total atmospheric column.

References

Adnashkin, V. N., L. K. Veselova, O. D. Barteneva, N. I. Nikitinskaya, and A. G. Laktionov, 1979: Atmospheric optical characteristics in the tropical zone of the Atlantic ocean (English translation). *Sov. Meteor. Hydrol.*, **N11**, 49–54.

Afonin, Y. I., 1983: Investigation on optical characteristics of maritime atmosphere (in Russian). *Abstracts, Third All-Union Conf. on Atmospheric Optics and Actinometry*, Part 1, Tomsk, Russia, Institute of Atmospheric Optics, 58–60.

Artemkin, E. E., and S. I. Krivoshein, 1983a: Statistical characteristics of atmospheric optical parameters over the water areas influenced by continent (in Russian). *Abstracts, Third All-Union Conf. on Atmospheric Optics and Actinometry*, Part 1, Tomsk, Russia, Institute of Atmospheric Optics, 277–279.

—, and —, 1983b: Statistical models of variability of the spectral structure of aerosol optical depths and polarization degrees of light scattered by the atmosphere over the background regions of the Atlantic ocean (in Russian). *Abstracts, Third All-Union Conf. on Atmospheric Optics and Actinometry*, Part 1, Tomsk, Russia, Institute of Atmospheric Optics, 274–276.

—, —, and S. G. Moiseev, 1980: Statistical characteristics of the spectral structure of aerosol optical depths (in Russian). *Abstracts, Second All-Union Conf. on Atmospheric Optics*, Part 1, Tomsk, Russia, Institute of Atmospheric Optics, 134–136.

Barteneva, O. D., L. K. Veselova, and N. I. Nikitinskaya, 1974: On the

- optical properties of atmospheric aerosols in the tropical zone of the Atlantic Ocean (in Russian). *Tropeks-72*, Gidrometeoizdat, 482–494.
- Blanchard, D. C., and A. H. Woodcock, 1980: The production, concentration, and vertical distribution of the sea-salt aerosol. *Ann. N. Y. Acad. Sci.*, **338**, 330–347.
- Bodhaine, B. A., B. G. Mendonca, J. M. Harris, and J. M. Miller, 1981: Seasonal variations in aerosols and atmospheric transmission at Mauna Loa Observatory. *J. Geophys. Res.*, **86**, 7395–7398.
- Brechtel, F. J., S. M. Kreidenweis, and H. B. Swan, 1998: Air mass characteristics, aerosol particle number concentrations, and number size distributions at Macquarie Island during the First Aerosol Characterization Experiment (ACE 1). *J. Geophys. Res.*, **103**, 16 351–16 367.
- Burmistrova, V. D., and G. L. Shubova, 1974: Aerosol atmospheric transmittance in tropical zones of the Atlantic and Pacific oceans (in Russian). *Hydrophysical and Hydrooptical Studies in the Atlantic and Pacific Oceans*, Nauka, 293–297.
- Charlson, R. J., S. E. Schwartz, J. M. Hales, R. D. Cess, J. A. Coakley Jr., J. E. Hansen, and D. J. Hofmann, 1992: Climate forcing by anthropogenic aerosols. *Science*, **255**, 423–430.
- Clarke, A. D., and J. N. Porter, 1994: Aerosol measurements and optical extinction in the marine boundary layer. *Proc., Int. Specialty Conf. on Aerosols and Atmospheric Optics: Radiative Balance and Visual Air Quality*, Vol. 4, Snowbird, UT, Air and Waste Management Association, 209–226.
- de Leeuw, G., 1991: Aerosol models for optical and IR propagation in the marine atmospheric boundary layer. *Proc. SPIE*, **1487**, 130–159.
- Deuze, J. L., C. Devaux, M. Herman, R. Santer, and D. Tanre, 1988: Saharan aerosols over the south of France: Characterization derived from satellite data and ground based measurements. *J. Appl. Meteor.*, **27**, 680–686.
- Eerme, K. A., 1983: Atmospheric and optical studies in the Baltic Sea from a board of research vessel *Ayu-Dag* in the summer of 1981 (in Russian).

- Studies of Variability of Optical Properties of the Baltic Sea*, Tallinn, 43–57.
- Emelyanov, V. N., S. L. Kislitsin, and S. A. Ilyicheva, 1978: Observations of spectral aerosol optical depths of atmosphere in the 28th cruise of research vessel *Professor Vize* (in Russian). *Aerosol Optics*, Ryazan, 23–28.
- Fischer, W. H., 1967: Some atmospheric turbidity measurements in Antarctica. *J. Appl. Meteor.*, **6**, 938–939.
- Fitzgerald, J. M., 1991: Marine aerosols: A review. *Atmos. Environ.*, **25A**, 533–545.
- Fraser, R. S., 1976: Satellite measurements of mass of Sahara dust in the atmosphere. *Appl. Opt.*, **15**, 2471–2479.
- Gashko, V. A., and K. S. Shifrin, 1983: Spectral transmittance of atmosphere in northwestern part of the Pacific Ocean (in Russian). *Marine Optics*, K. S. Shifrin, Ed., Nauka, 190–194.
- Gathman, S. G., 1983: Optical properties of the marine aerosol as predicted by the Navy aerosol model. *Opt. Eng.*, **22**, 57–62.
- Gras, J. L., 1995: CN, CNN and particle size in Southern Ocean air at Cape Grim. *Atmos. Res.*, **35**, 233–251.
- Guschin, G. K., 1970: Optical characteristics of aerosols over the oceans (in Russian). *Tr. Gl. Geofiz. Obs.*, **255**, 52–68.
- Guttman, A., 1968: Extinction coefficient measurements of clear atmospheres and cirrus clouds. *Appl. Opt.*, **7**, 2377–2381.
- Haggerty, J. A., P. A. Durkee, and B. J. Wattle, 1990: A comparison of surface and satellite-derived aerosol measurements in the western Mediterranean. *J. Geophys. Res.*, **95**, 1547–1557.
- Hansen, J., M. Sato, and R. Ruedy, 1997: Radiative forcing and climate response. *J. Geophys. Res.*, **102**, 6831–6864.
- , —, —, A. Lacis, and V. Oinas, 2000: Global warming in the twenty-first century: An alternative scenario. *Proc. Natl. Acad. Sci. U.S.A.*, **97**, 9875–9880.
- Hayasaka, T., N. Iwasaka, G. Hashida, I. Takizawa, and M. Tanaka, 1994: Changes in stratospheric aerosols and solar insolation due to Mt. Pinatubo eruption as observed over

- the western Pacific. *Geophys. Res. Lett.*, **21**, 1137–1140.
- Herman, J., P. K. Bhartia, O. Torres, N. C. Hsu, C. J. Seftor, and E. Celarier, 1997: Global distribution of UV-absorbing aerosols from Nimbus 7/TOMS data. *J. Geophys. Res.*, **102**, 16 911– 16 921.
- Hess, M., P. Koepke, and I. Schult, 1998: Optical properties of aerosols and clouds: The software package OPAC. *Bull. Amer. Meteor. Soc.*, **79**, 831–844.
- Hogan, A. W., 1981: Aerosol measurements over and near the south Pacific Ocean and Ross Sea. *J. Appl. Meteor.*, **20**, 1111–1118.
- Holben, B. N., and Coauthors, 1998: AERONET—A federated instrument network and data archive for aerosol characterization. *Remote. Sens. Environ.*, **66**, 1–16.
- , and Coauthors, 2001: An emerging ground based aerosol climatology: Aerosol optical depth from AERONET. *J. Geophys. Res.*, **106**, 12 067–12 097.
- Hoppel, W. A., and G. M. Frick, 1990: Submicron aerosol size distributions measured over the tropical and South Pacific. *Atmos. Environ.*, **24A**, 645–659.
- , J. W. Fitzgerald, and R. E. Larson, 1985: Aerosol size distributions in air masses advecting off the East Coast of the United States. *J. Geophys. Res.*, **90**, 2365–2379.
- , —, G. M. Frick, R. E. Larson, and E. J. Mack, 1990: Aerosol size distributions and optical properties found in the marine boundary layer over the Atlantic Ocean. *J. Geophys. Res.*, **95**, 3659–3686.
- Horvath, H., R. L. Gunter, and S. W. Wilkinson, 1990: Determination of the coarse mode of the atmospheric aerosol using data from a forward-scattering spectrometer probe. *Aerosol Sci. Technol.*, **12**, 964–980.
- Husar, R. B., J. M. Prospero, and L. L. Stowe, 1997: Characterization of tropospheric aerosols over the oceans with the NOAA advanced very high resolution radiometer optical thickness operational product. *J. Geophys. Res.*, **102**, 16 889–16 909.
- Ignatov, A. M., I. L. Dergileva, S. M. Sakerin, and D. M. Kabanov, 1993: An algorithm for the sun photometer calibration. *Proc. IGARSS' 93*

- Symp.*, Tokyo, Japan, IEEE, 1091–1093.
- IPCC, 1994: *Radiative Forcing of Climate*. Cambridge University Press.
- Jaenicke, R., and L. Schutz, 1978: Comprehensive study of physical and chemical properties of the surface aerosol in the Cape Verde islands region. *J. Geophys. Res.*, **83**, 3585–3599.
- Jankowiak, I., and D. Tanre, 1992: Satellite climatology of Saharan dust outbreaks: Method and preliminary results. *J. Climate*, **5**, 646–656.
- Jennings, S. G., and C. D. O'Dowd, 1990: Volatility of aerosol at Mace Head, on the west coast of Ireland. *J. Geophys. Res.*, **95**, 13 937–13 948.
- Kuznetsov, G. I., and N. I. Izhovkina, 1973: Two models of atmospheric aerosol (English translation). *Izv. Acad. Sci. USSR Atmos. Oceanic Phys.*, **9**, 537–540.
- Livingston, J. M., and Coauthors, 2000: Shipboard sunphotometer measurements of aerosol optical depth spectra and columnar water vapor during ACE-2 and comparison with selected land, ship, aircraft, and satellite measurements. *Tellus*, **52B**, 593–618.
- Lukyanchikova, N. A., and A. A. Govorushkin, 1981: Spectral characteristics of atmosphere over the northern part of the Atlantic Ocean (in Russian). *Tr. Arct. Antarct. Inst.*, **370**, 160–164.
- Masuda, K., M. Sasaki, T. Takashima, and H. Ishida, 1999: Use of polarimetric measurements of the sky over the ocean for spectral optical thickness retrievals. *J. Atmos. Oceanic Technol.*, **16**, 846–859.
- Mather, J. H., T. P. Ackerman, W. E. Clements, F. J. Barnes, M. D. Ivey, L. D. Hatfield, and R. M. Reynolds, 1998: An atmospheric radiation and cloud station in the tropical western Pacific. *Bull. Amer. Meteor. Soc.*, **79**, 627–642.
- Matsubara, K., T. Ohata, and S. Kawaguchi, 1983: Turbidity over the Indian Ocean. *Proceedings of the Fifth Symposium on Polar Meteorology and Glaciology*, Special Issue 29, Memoirs of the National Institute of Polar Research, 77–84.
- Zibordi, G., and G. Maracci, 1988: Determination of atmospheric



turbidity from remotely-sensed data:

A case study. *Int. J. Remote Sens.*,

9, 1881–1894.

